Science
AAAS

Supplementary Materials for

A protein interaction landscape of breast can

Minkyu Kim *et al.*

Corresponding authors: Trey Ideker, nevan.krogan@ucsf.edu; Nevan J. Krogan, tideker@ucsd.edu

Science **374**, eabf3066 (2021)
DOI: 10.1126/science.abf3066

The PDF file includes:

Other Supplementary Material for this manuscript includes the following:

Supplementary Text

Primary Antibody used for PLA:

Antibody	**Cat#**	**Dilution**	**Antibody**	**Cat#**	**Dilution**
HRAS	Proteintech 18295-1-AP	1:200	FANCI	Santa Cruz sc-271316	1:200
STK11	Santa Cruz sc-32245	1:200	MMS19	Proteintech 16015-1-AP	1:200
PIK3CA	Invitrogen MA5-17149	1:400	BPIFA1	Abcam ab131163	1:400
FLAG M2	Sigma F3165	1:1000			

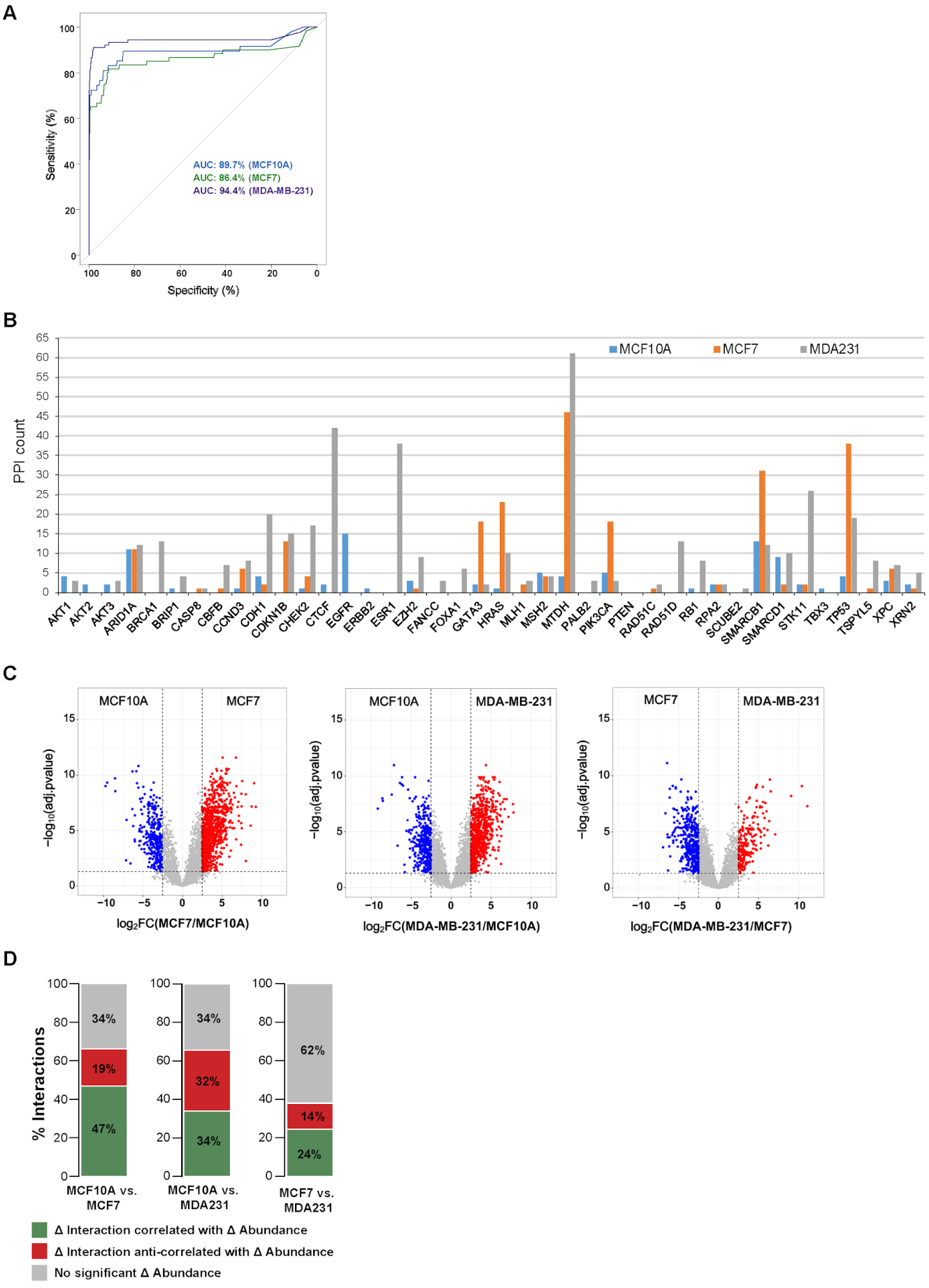
A
Sensitivity (%)
Specificity (%)
AUC: 89.7% (MCF10A)
AUC: 86.4% (MCF7)
AUC: 94.4% (MDA-MB-231)
B
PPI count
MCF10A
MCF7
MDA231
AKT1 AKT2 AKT3 ARID1A BRCA1 BRIP1 CASP8 CBFB CCND3 CDH1 CDKN1B CHEK2 CTCF EGFR ERBB2 ESR1 EZH2 FANCC FOXA1 GATA3 HRAS MLH1 MSH2 MTDH PALB2 PIK3CA PTEN RAD51C RAD51D RB1 RPA2 SCUBE2 SMARCB1 SMARCD1 STK11 TBX3 TP53 TSPYL5 XPC XRN2
C
MCF10A
MCF7
MDA-MB-231
−log10(adj.pvalue)
log2FC(MCF7/MCF10A)
log2FC(MDA-MB-231/MCF10A)
log2FC(MDA-MB-231/MCF7)
D
% Interactions
34%
19%
47%
34%
32%
34%
62%
14%
24%
MCF10A vs. MCF7
MCF10A vs. MDA231
MCF7 vs. MDA231
Δ Interaction correlated with Δ Abundance
Δ Interaction anti-correlated with Δ Abundance
No significant Δ Abundance

Fig. S1. Overview of high-confidence PPIs from three breast cell lines.

(**A**) Receiver operating characteristic (ROC) curve illustrating high recovery of gold standards (sensitivity). (**B**) Number of high-confidence PPIs per cell line for each bait. (**C**) Volcano plots displaying the differential abundance of endogenous proteins between cell lines used in this study. Colored data points indicate proteins that have ≥ 5.6-fold difference in protein abundance between cell lines and an adjusted p-value ≤ 0.05. (**D**) Percentage of unique interactions (preys) for the same bait between cell lines with a correlated (green) or anticorrelated (red) significant change (≥ 2-fold change, adjusted p-value ≤ 0.05) in abundance. Gray indicates unique interactions with no significant change in abundance. Only preys detected by global abundance mass spectrometry analysis are considered.

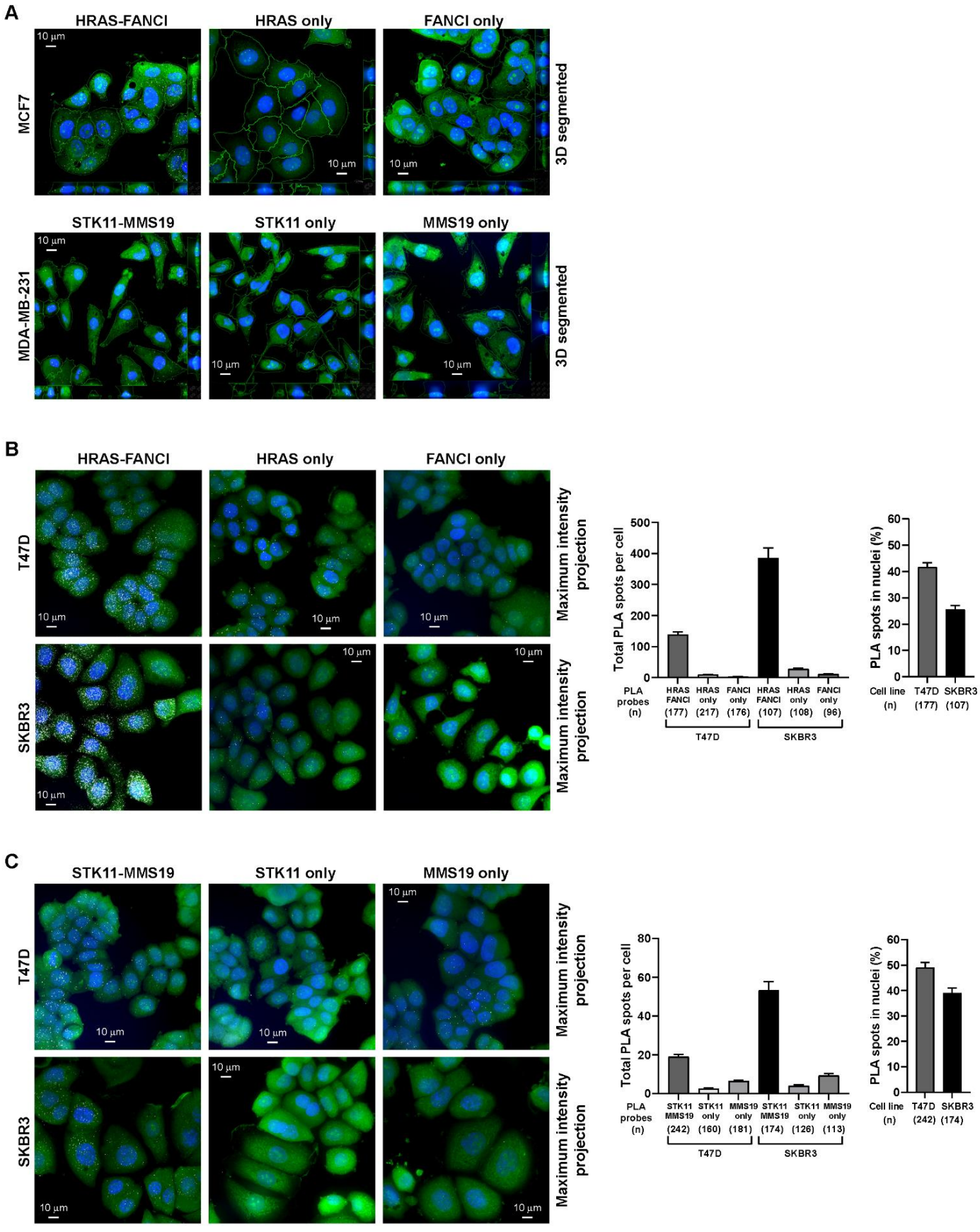
A
HRAS-FANCI
HRAS only
FANCI only
MCF7
3D segmented
STK11-MMS19
STK11 only
MMS19 only
MDA-MB-231
3D segmented
10 µm
B
HRAS-FANCI
HRAS only
FANCI only
T47D
Maximum intensity projection
SKBR3
Maximum intensity projection
Total PLA spots per cell
PLA probes (n)
HRAS FANCI (177)
HRAS only (217)
FANCI only (176)
HRAS FANCI (107)
HRAS only (108)
FANCI only (96)
T47D
SKBR3
PLA spots in nuclei (%)
Cell line (n)
T47D (177)
SKBR3 (107)
C
STK11-MMS19
STK11 only
MMS19 only
T47D
Maximum intensity projection
SKBR3
Maximum intensity projection
Total PLA spots per cell
PLA probes (n)
STK11 MMS19 (242)
STK11 only (160)
MMS19 only (181)
STK11 MMS19 (174)
STK11 only (126)
MMS19 only (113)
T47D
SKBR3
PLA spots in nuclei (%)
Cell line (n)
T47D (242)
SKBR3 (174)

Fig. S2. Validation of the HRAS-FANCI and STK11-MMS19 interactions by proximity ligation assay.

(**A**) Examples of 3D segmented images with a single XY slice and corresponding orthogonal views showing representations of Z planes for the HRAS-FANCI PLA in MCF7 (top row) and the STK11-MMS19 PLA in MDA-MB-231 (bottom row). PLA with only one of the two primary antibodies was performed as negative control (middle and right column). PLA spots (white), HCS CellMask Green stain (green) and DAPI (blue). (**B**) Representative maximum intensity projection images of T47D (top row) and SKBR3 (bottom low) cells from the PLA between HRAS and FANCI antibodies. (**C**) Representative maximum intensity projection images of T47D (top row) and SKBR3 (bottom low) cells from the PLA between STK11 and MMS19 antibodies. Total PLA spots per cell and percent nuclear PLA spots in each PLA condition were quantified. *n* indicates the total number of cells analyzed in each condition. Scale bar, 10 μm.

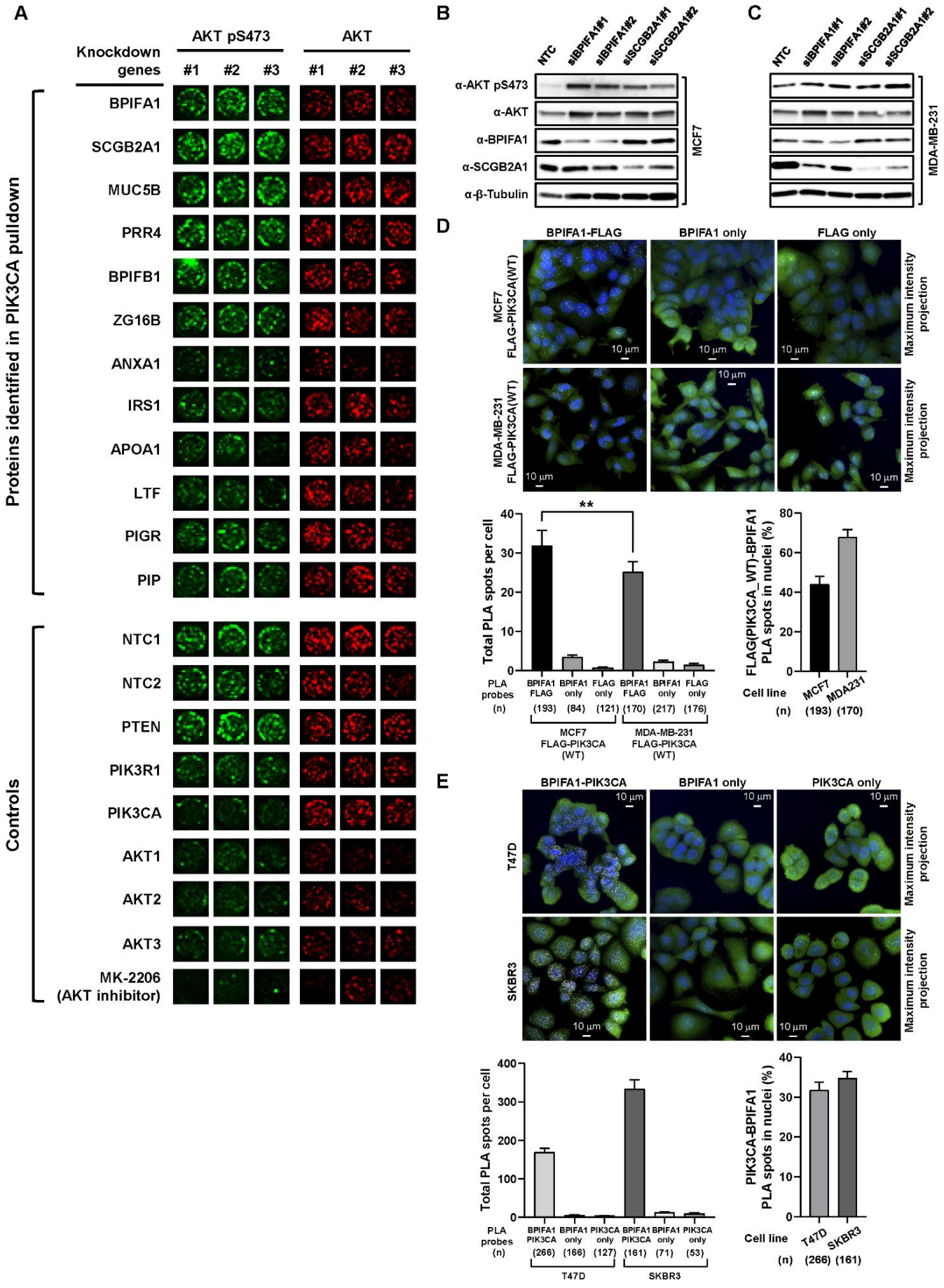
A
Knockdown genes
AKT pS473
AKT
#1
#2
#3
Proteins identified in PIK3CA pulldown
BPIFA1
SCGB2A1
MUC5B
PRR4
BPIFB1
ZG16B
ANXA1
IRS1
APOA1
LTF
PIGR
PIP
Controls
NTC1
NTC2
PTEN
PIK3R1
PIK3CA
AKT1
AKT2
AKT3
MK-2206 (AKT inhibitor)
B
NTC
siBPIFA1#1
siBPIFA1#2
siSCGB2A1#1
siSCGB2A1#2
α-AKT pS473
α-AKT
α-BPIFA1
α-SCGB2A1
α-β-Tubulin
MCF7
C
MDA-MB-231
D
BPIFA1-FLAG
BPIFA1 only
FLAG only
MCF7 FLAG-PIK3CA(WT)
MDA-MB-231 FLAG-PIK3CA(WT)
Maximum intensity projection
10 μm
Total PLA spots per cell
PLA probes
(n)
BPIFA1 FLAG
BPIFA1 only
FLAG only
(193)
(84)
(121)
(170)
(217)
(176)
MCF7 FLAG-PIK3CA (WT)
MDA-MB-231 FLAG-PIK3CA (WT)
FLAG(PIK3CA_WT)-BPIFA1 PLA spots in nuclei (%)
Cell line
MCF7
MDA231
E
BPIFA1-PIK3CA
BPIFA1 only
PIK3CA only
T47D
SKBR3
PIK3CA
(266)
(166)
(127)
(161)
(71)
(53)
PIK3CA-BPIFA1 PLA spots in nuclei (%)

Fig. S3. Physical and functional interaction of PIK3CA with BPIFA1 and SCGB2A1.

(**A**) Small interfering RNA-mediated knockdown of genes identified in PIK3CA pulldown was performed in MCF7 using 96-well plates. Levels of phosphorylated AKT on S473 and total AKT following knockdown in each well were measured by in-cell western analysis. Three representative well images out of 9 replicates for both AKT pS473 and total AKT are shown. (**B-C**) The effect of BPIFA1 and SCGB2A1 knockdown on the level of pAKT (S473) was confirmed by two individual siRNAs in MCF7 and MDA-MB-231 cells, respectively. (**D**) The association of FLAG-tagged PIK3CA (WT) with BPIFA1 was confirmed by PLA in MCF7 and MDA-MB-231 cells bearing 3xFLAG-PIK3CA transgene using anti-FLAG and anti-BPIFA1 antibodies. Representative maximum intensity projection images of MCF7 (top row) and MDA-MB-231 (bottom low) cells are shown. (**E**) The PIK3CA-BPIFA1 interaction was also observed by PLA in T47D and SKBR3 cells using anti-PIK3CA and anti-BPIFA1 antibodies. Representative maximum intensity projection images of T47D (top row) and SKBR3 (bottom low) cells are shown. Total PLA spots per cell and percent nuclear PLA spots in each PLA condition were quantified. *n* indicates the total number of cells analyzed in each condition. Scale bar, 10 μm.

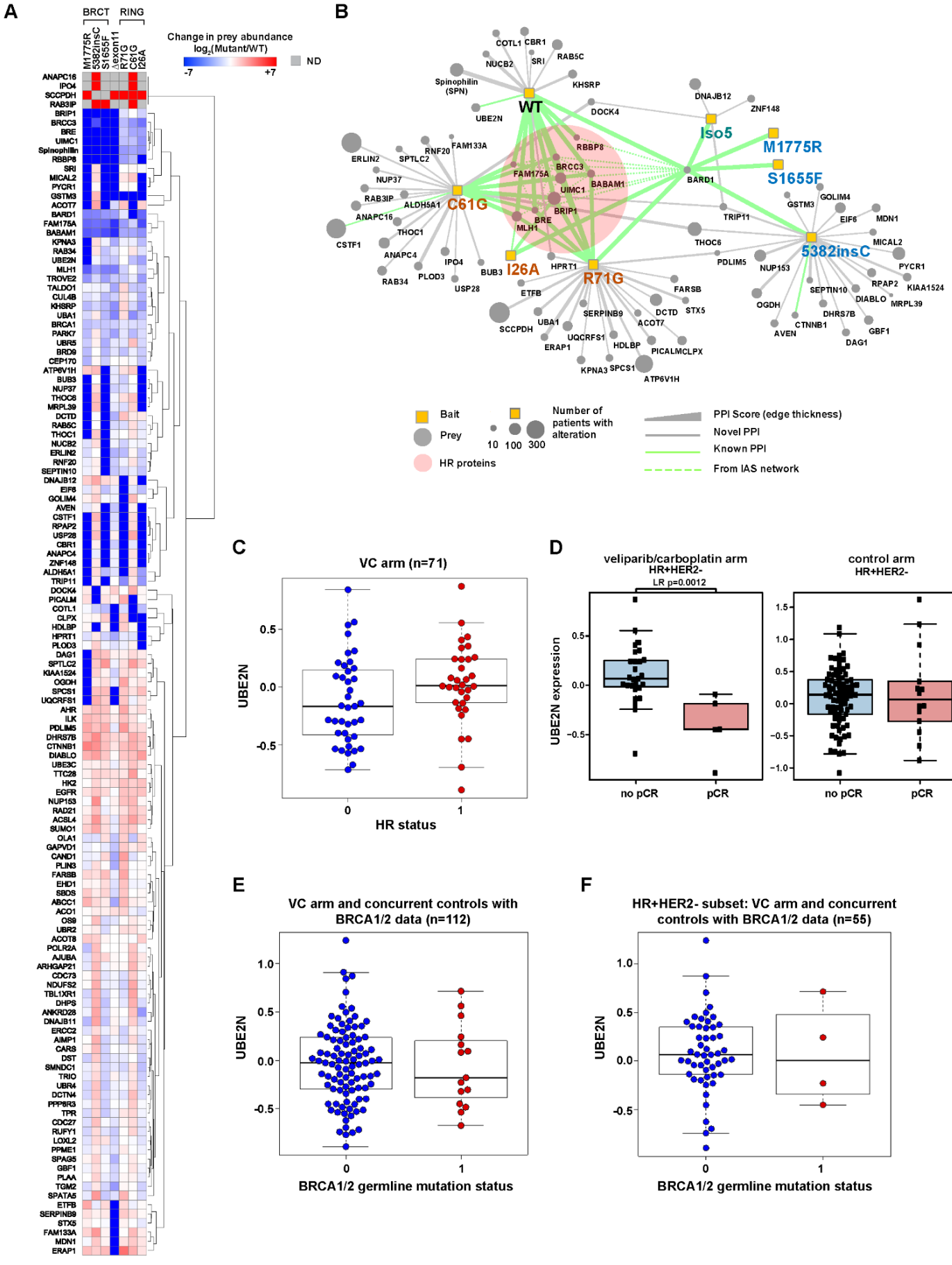
A
BRCT
RING
M1775R
5382insC
S1655F
Δexon11
R71G
C61G
I26A
Change in prey abundance
log2(Mutant/WT)
-7
+7
ND
B
WT
Iso5
M1775R
S1655F
5382insC
C61G
I26A
R71G
Bait
Prey
HR proteins
Number of patients with alteration
10 100 300
PPI Score (edge thickness)
Novel PPI
Known PPI
From IAS network
C
VC arm (n=71)
UBE2N
HR status
D
veliparib/carboplatin arm
HR+HER2-
LR p=0.0012
control arm
HR+HER2-
UBE2N expression
no pCR
pCR
E
VC arm and concurrent controls with BRCA1/2 data (n=112)
UBE2N
BRCA1/2 germline mutation status
F
HR+HER2- subset: VC arm and concurrent controls with BRCA1/2 data (n=55)
UBE2N
BRCA1/2 germline mutation status

Fig. S4. Pathogenic mutations in the BRCT domain of BRCA1 disrupt the interaction with HR proteins.

(**A**) Relative quantification of the abundance of prey proteins (PPI score ≥ 0.65) identified by BRCA1 AP-MS in MDA-MB-231 cells. Preys detected only in wild type are represented in deep blue, and preys detected only in mutants are in deep red. ND, not detected. (**B**) PPIs across all BRCA1 proteins analyzed (the wild type and 7 mutants) are visualized in a network view. A selective set of prey proteins (PPI score ≥ 0.65, ≥ 8-fold change) is shown. Proteins playing crucial roles in DNA repair by homologous recombination are circled in pink. (**C**) Although the average expression of UBE2N is numerically lower in TN than HR+HER2- tumors, the difference is not statistically significant ($P = 0.1$). (**D**) Association of low UBE2N expression to pCR to VC is seen significantly in the HR+HER2- subset (p=0.0012) while there is no significant difference in UBE2N expression between pCR and no-pCR groups in the control arm. (**E**) UBE2N trends toward lower expression levels in BRCA1/2 mutation carriers ($P = 0.07$). (**F**) In the HR+HER2- subset (n = 55 with BRCA1/2 mutation data), where lower UBE2N levels associate with response to VC, there are only 4 mutation carriers and no difference in UBE2N levels by BRCA1/2 status ($P = 1$).

A

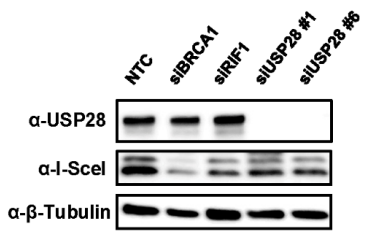

B

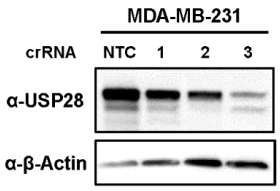

C

275 proteins (319 ub-peptides): UP GO terms [log_2FC(crRNA#3/NTC) ≥ 1]	p-value	FDR	# of Proteins
translational elongation (GO:0006414)	1.91E-10	4.18E-07	20
protein folding (GO:0006457)	4.73E-06	7.36E-04	9
protein polyubiquitination (GO:0000209)	4.27E-05	3.45E-03	9
cellular response to stress (GO:0033554)	5.84E-05	4.55E-03	19
cellular protein-containing complex assembly (GO:0034622)	1.55E-04	1.02E-02	16
organelle organization (GO:0006996)	1.89E-04	1.22E-02	46
ribosomal large subunit biogenesis (GO:0042273)	2.43E-04	1.47E-02	6
protein-DNA complex subunit organization (GO:0071824)	2.71E-04	1.60E-02	8
proteasome-mediated ubiquitin-dependent protein catabolic process (GO:0043161)	3.71E-04	2.02E-02	10
regulation of mRNA metabolic process (GO:1903311)	6.84E-04	3.47E-02	7
ribosomal subunit export from nucleus (GO:0000054)	7.24E-04	3.51E-02	3
cytoplasmic translation (GO:0002181)	1.04E-03	4.53E-02	5

72 proteins (76 ub-peptides): DOWN GO terms [log_2FC(crRNA#3/NTC) ≤ -1]	p-value	FDR	# of Proteins
viral life cycle (GO:0019058)	1.20E-07	1.58E-04	9
translational initiation (GO:0006413)	9.15E-07	7.60E-04	7
SRP-dependent cotranslational protein targeting to membrane (GO:0006614)	1.50E-06	1.12E-03	6
viral transcription (GO:0019083)	4.25E-06	2.48E-03	6
nuclear-transcribed mRNA catabolic process, nonsense-mediated decay (GO:0000184)	5.12E-06	2.79E-03	6
regulation of cellular metabolic process (GO:0031323)	1.36E-04	3.36E-02	37
positive regulation of protein insertion into mitochondrial membrane involved in apoptotic signaling pathway (GO:1900740)	1.39E-04	3.32E-02	3
ribosomal large subunit assembly (GO:0000027)	1.70E-04	3.72E-02	3
regulation of primary metabolic process (GO:0080090)	1.95E-04	4.22E-02	36

D

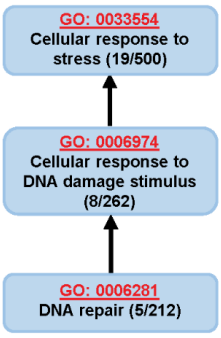

E

Cellular response to stress (GO: 0033554)			
Protein	Ub-site	Protein	Ub-site
BAG6	K80	MCM6	K197
DDB2	K163	PAK2	K138
EGLN1	K400	PML	K400
FXR1	K207	PSMC6	K206
HNRNPM	K651	RAD18	K318
HSP90AA1	K112, K283, K489, K632	TRAF1	K76
HSPA1B	K451, K539, K507	TRAF2	K255
HSPA8	K128	UBA1	K470
HSPD1	K125	WRNIP1	K482
MCM3	K435		

Fig. S5. USP28 knockdown reveals various proteins potentially deubiquitinated by USP28.

(**A**) USP28 knockdown in U2OS DR-GFP reporter cells by siRNAs was confirmed by western blot analysis and decreases HR activity as seen in Fig. 4G. (**B**) Knockdown of USP28 in MDA-MB-231 cells by three independent CRISPR-Cas9 RNPs was monitored by Western blot. A pool of USP28 knockdown cells by crRNA3 was subsequently used for Ub-proteomic analysis. (**C**) Significant (FDR < 0.05) Gene Ontology (PANTHER GO Slim Biological Process) terms for significantly up (top) and down-regulated (bottom) ubiquitinated proteins following USP28 knockdown. (**D**) Gene Ontology hierarchy of significant terms related to cellular response to stress, cellular response to DNA damage stimulus, and DNA repair using PANTHER GO Slim database. (**E**) Up-regulated Ub-sites on proteins which belong to cellular response to stress Gene Ontology term are listed.

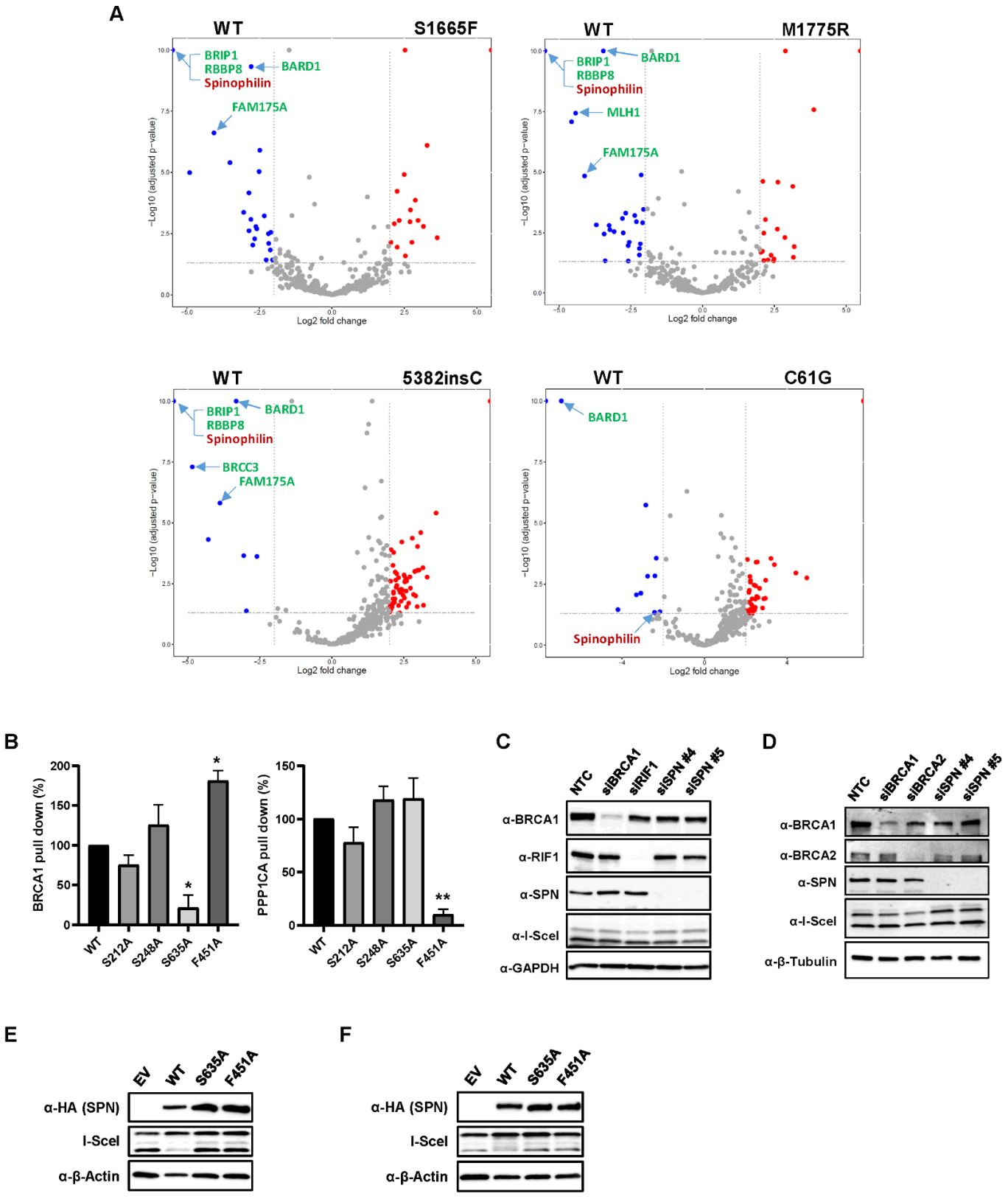

Fig. S6. Physical and functional validation of the BRCA1-SPN interaction.

(**A**) Volcano plots show proteins that differentially interact with BRCA1 between wild type and mutants. The BRCT domain mutations tested (S1655F, M1775R, and 5382insC) completely abolish the interaction of BRCA1 with spinophilin as well as BRIP1 and RBBP8, whereas C61G mutation in the RING domain abrogates the interaction with BARD1. Colored data points indicate proteins that have ≥ fourfold difference in protein interaction between WT and mutants and an adjusted $P \leq 0.05$. (**B**) The levels of BRCA1 and PPP1CA pulled down with HA-tagged SPN (WT, S212A, S248A, S635A, and F451A) were quantified from three independent experiments after normalization to SPN and input signals. * $P \leq 0.05$, ** $P \leq 1.0 \times 10^{-2}$. (**C**) Levels of BRCA1, RIF1, SPN, I-SceI and GAPDH proteins in U2OS/DR-GFP cells following knockdown were analyzed by Western blot. (**D**) Levels of BRCA1, BRCA2, SPN, I-SceI and **β**-tubulin proteins in U2OS/SA-GFP cells following knockdown were analyzed by Western blot. (**E**) Levels of SPN (WT, S635A, and F451A), I-SceI, and **β**-actin proteins in U2OS/DR-GFP cells following transfection were analyzed by Western blot. (**F**) Levels of SPN (WT, S635A, and F451A), I-SceI, and **β**-actin proteins in U2OS/SA-GFP cells following transfection were analyzed by Western blot.

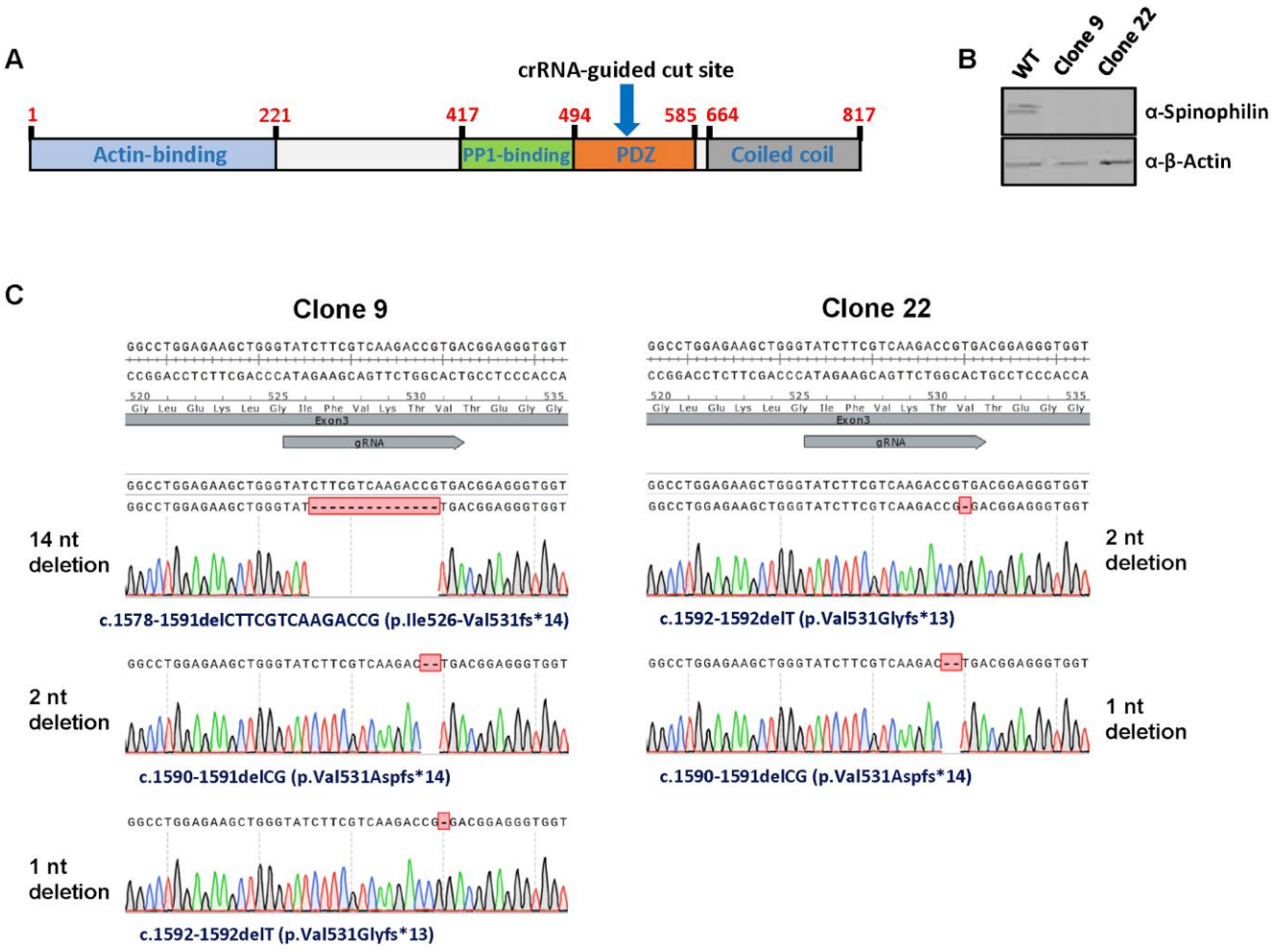

Fig. S7. Generation and verification of *PPP1R9B* (encoding spinophilin) knockout clones.

(**A**) Functional domains/motifs in the *PPP1R9B* gene and the location of CRISPR-Cas9-mediated cut site to introduce INDELS to generate knockout (KO) clones. (**B**) Confirmation of knockout by western blot analysis using α-Spinophilin (SPN) antibody. (**C**) Exome sequencing verified disruption of *PPP1R9B* alleles in two knockout clones (9 and 22).

A

Peptide substrate	Residue	Known kinase	Parental Run#1	Parental Run#2	SPN KO Run#1	SPN KO Run#2	Net peptide phosphorylation	p-value
LIMK2	T526	CDC42BPA; ROCK1	-68.96	-32.55	33.76	67.75	101.50	0.028
MYC	T58	GSK3B; CSNK2A1; CSNK2A2	-38.18	-34.70	29.57	43.31	72.88	0.005
FOXO1	S256	AKT1; PAK1	-45.54	-14.37	21.30	38.61	59.91	0.039
RPS6KA1	S221	PDPK1	-33.41	-23.59	10.24	46.76	57.00	0.047
CRK	Y221	ABL1; ABL2; EGFR; IGF1R	-34.43	-16.64	21.07	30.00	51.07	0.018
JAK1	Y1034	JAK3; JAK1	-9.68	-40.25	30.84	19.09	49.93	0.046
BRCA1	T509	AKT1	-33.87	-14.94	25.03	23.77	48.81	0.018
BRCA1	S1387	ATM; ATR	-19.34	-22.99	7.79	34.54	42.33	0.044
MTOR	S2481	MTOR	-23.23	-14.87	28.31	9.79	38.10	0.032
AKT1 / AKT2 / AKT3	T308 / T309 / T305	CAMKK1; IKBKE; PDK1; PDPK1; PRKCA; PRKCB; PRKCZ	-29.56	-5.81	17.30	18.07	35.37	0.048
NFKB1	S923	CHUK; IKBKB	-11.10	-24.24	9.64	25.70	35.34	0.038
NFKBIB	S23	CHUK; IKBKB	-21.37	-11.25	10.53	22.09	32.62	0.026
MTOR	T2446	AKT1; AKT3; RPS6KB1	-20.21	-7.76	8.56	19.41	27.97	0.039
MAP2K1 / MAP2K2	S222 / S226	ARAF; BRAF; RAF1; MAP3K1; MAP3K8; PDPK1	-21.33	-6.54	8.95	18.93	27.88	0.044
BRCA1	S1423	ATM; ATR	-8.74	-13.36	8.20	13.90	22.09	0.013
H2AX	S140	ATM	-7.84	-13.64	10.59	10.89	21.48	0.009
SMAD2	S250	MAPK1; MAPK3	-7.83	-12.52	11.32	9.04	20.36	0.008
CDKN1A	T145	AKT1; DAPK3; PIM1	-4.37	-15.55	6.86	13.06	19.92	0.045
TP53	T55,E56K	MAPK1	-12.11	-6.61	11.41	7.31	18.72	0.016
RAF1	Y341	SRC; JAK2	-6.34	-11.65	6.27	11.73	18.00	0.021
INCENP	T892,S893,S894	AURKB	2.72	-1.47	-1.31	0.05	-1.25	0.313
BCAR1	Y234	SRC	3.85	-1.66	-3.53	1.34	-2.19	0.306

B

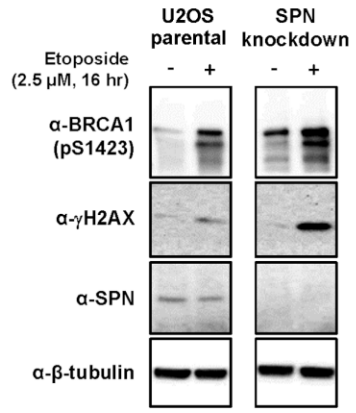

Fig. S8. Knockout of *PPP1R9B* (encoding spinophilin) upregulates phosphorylation on BRCA1 and H2AX.

(**A**) Top 20 most increased phosphosites in SPN KO cell lysates, compared to parental MDA-MB-231 cell lysates. Net phosphorylation of the peptides derived from 237 proteins including BRCA1 and H2AX was calculated based on ATP consumption between SPN KO and parental cell lysates. Peptides from INCENP and BCAR1 are shown as unaffected controls. Kinase(s) known to phosphorylate each phosphosite is also listed. The numbers from each run are plate median-normalized ATP concentrations remaining in each well after reaction (mixed with extracts). Net phosphorylation values are net changes in ATP concentrations between SPN knockout cells and parental control cells (subtraction of parental runs from SPN KO runs). Mean value of two independent runs was shown. Units are arbitrary. (**B**) Accumulation of BRCA1 pS1423 and γ-H2AX in SPN KO cells were validated by Western blot analysis in the absence or presence of etoposide (2.5 μM, 16 hours) treatment.

A

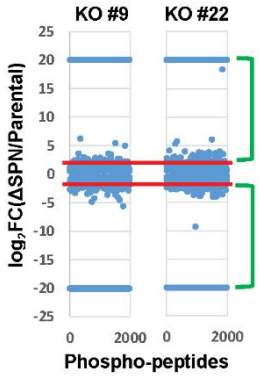

B

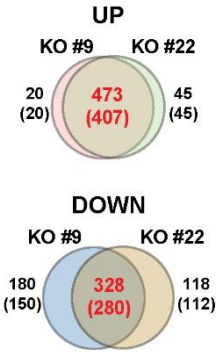

C

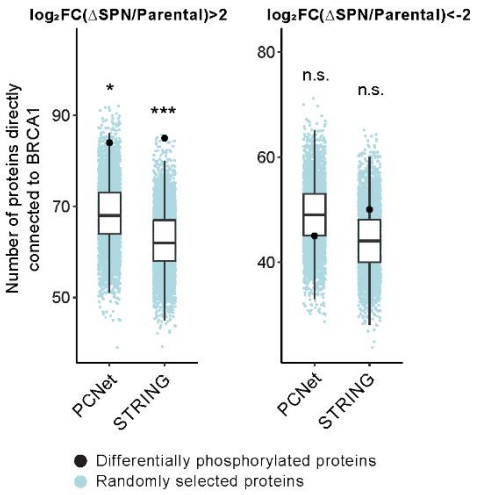

D

UP GO terms [log_2FC(ΔSPN/Parental) > 2]	p-value	FDR
cytoskeleton organization	1.74E-05	6.25E-03
regulation of supramolecular fiber organization	8.04E-05	1.44E-02
mRNA cis splicing, via spliceosome	1.66E-04	2.30E-02
DNA repair	2.81E-04	3.37E-02
regulation of mRNA processing	3.34E-04	3.53E-02
mitotic cell cycle process	4.14E-04	3.54E-02
cellular component biogenesis	5.31E-04	3.81E-02
negative regulation of transcription by RNA polymerase II	5.80E-04	4.00E-02
regulation of microtubule polymerization or depolymerization	5.97E-04	3.97E-02

DOWN GO terms [log_2FC(ΔSPN/Parental) < -2]	p-value	FDR
transcription by RNA polymerase II	4.01E-07	2.40E-04
regulation of transcription by RNA polymerase II	1.11E-05	1.82E-03
mRNA processing	1.30E-05	1.94E-03

E

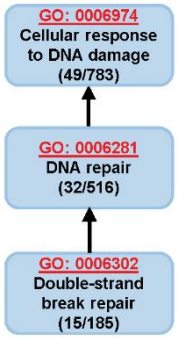

F

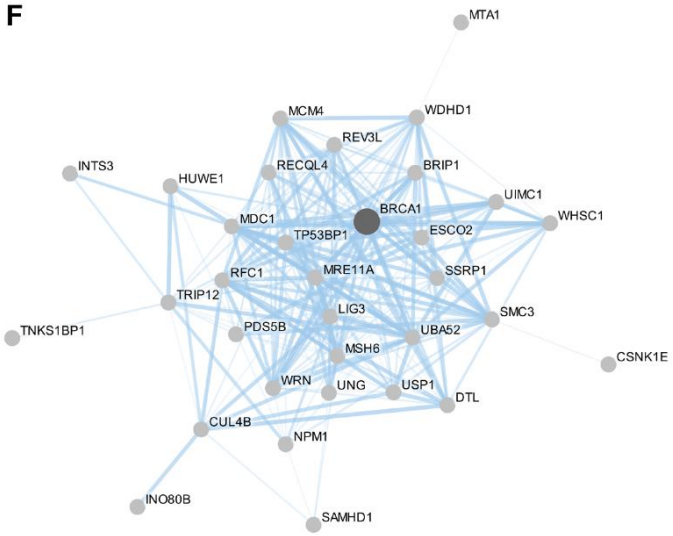

G

Protein	Phospho-site	Protein	Phospho-site
BRIP1	S990	RECQL4	S323
CSNK1E	S363	REV3L	S1967
CUL4B	S193	RFC1	S368, S520
DTL	S679	SAMHD1	S18, T21
ESCO2	S223	SMC3	S1074
HUWE1	T3924, T3927	SSRP1	S671
INO80B	S63	TNKS1BP1	S1533, S1652
INTS3	S995	TP53BP1	S379
LIG3	S227	TRIP12	S991
MCM4	S31	UBA52	S65
MDC1	S1086	UIMC1	S463
MRE11A	S678, S688	UNG	T60, S64
MSH6	S309	USP1	S16, S292
MTA1	S522	WDHD1	S1090
NPM1	S88	WHSC1	T110, T115, S177
PDS5B	T1370	WRN	S1133

Fig. S9. Phospho-proteomic analysis reveals phosphorylation sites on various DNA repair proteins that are accumulated in spinophilin (SPN) KO cells.

(**A**) Phospho-proteomes of the two SPN knockout clones (9 and 22) and parental MDA-MB-231 cells were analyzed. $Log_2FC(\Delta SPN/Parental)$ was plotted for phospho-peptides detected at least in two biological replicates with p-value ≤ 0.05. Red lines denote $Abs[log_2FC(\Delta SPN/Parental)] = 2$ cut-off and green brackets include phosphopeptides either 4-fold up or down-regulated in SPN KO cells. (**B**) Overlap of 4-fold up or down-regulated phospho-peptides between the two SPN KO clones. Numbers of phospho-peptides are shown. Numbers in parentheses are for corresponding proteins. (**C**) The interconnectedness of the 4-fold up (left) or down (right)-regulated proteins to BRCA1 (number of connections to BRCA1) was determined using either PCNet or STRING networks (black dots) and compared to 5000 random selections of equally-sized sets of proteins (blue dots) to calculate an empirical p-value. * $P \leq 0.05$, *** $P \leq 1.0 \times 10^{-3}$, n.s. (not significant). (**D**) Significant (FDR < 0.05) Gene Ontology (PANTHER GO Slim Biological Process) terms for significantly up (top) and down-regulated (bottom) phosphorylated proteins following SPN KO. (**E**) Gene Ontology hierarchy of significant terms related to DNA damage response using full PANTHER GO database (not Slim). (**F**) Subnetwork of enriched proteins from the DNA repair term (32 proteins) from the STRING network. Although BRCA1 phospho-sites were not detected in phospho-proteomic analysis, BRCA1 was added in the network to visualize interconnectedness of regulated proteins with BRCA1, based on peptide phosphorylation assay. (**G**) Phospho-sites on the 32 DNA repair proteins that were accumulated in SPN KO cells are listed.

Table S1. Key resources used in the study

REAGENT	SOURCE	IDENTIFIER
Antibodies		**Cat#**
HRAS	Proteintech	18295-1-AP
FANCI	Santa Cruz Biotechnology	sc-271316
MMS19	Proteintech	16015-1-AP
STK11 (Ley 37D/G6)	Santa Cruz Biotechnology	sc-32245
STK11	Cell Signaling Technologies	3050
pSTK11	Cell Signaling Technologies	3482
pAMPK	Cell Signaling Technologies	2535
AMPK	Cell Signaling Technologies	5832
pSIKs	Abcam	ab199474
SIK1	Thermo Fisher Scientific	PA5-42799
SIK2	Cell Signaling Technologies	6919S
Vinculin	Cell Signaling Technologies	13901S
Phospho-AKT (Ser473) (D9E) XP Rabbit mAb	Cell Signaling Technologies	4060S
Akt (pan)(40D4) Mouse mAb	Cell Signaling Technologies	2920S
Goat Anti-Mouse Secondary Antibody 800CW LI-COR	LI-COR	926-32210
Goat Anti-Rabbit Secondary Antibody 800CW LI-COR	LI-COR	926-32211
BPIFA1	Abcam	ab131163
SCGB2A1	Invitrogen	PA5-56981
FLAG (M2)	Sigma-Aldrich	F3165
PIK3CA	Invitrogen	MA5-17149
Beta-Tubulin	Sigma-Aldrich	T8328
Actin (13E5)	Cell Signaling Technologies	4970
PIK3CA (C73F8)	Cell Signaling Technologies	4249S
PTEN	Cell Signaling Technologies	9552S
Anti-Mouse IgG, HRP-linked	Cell Signaling Technologies	7076
Anti-Rabbit IgG, HRP-linked	Cell Signaling Technologies	7074
BRCA1 (D-9)	Santa Cruz Biotechnology	sc-6954
BRCA1	EMP Millipore	OP92
BRCA1 pS1423	Bethyl Laboratories	A300-008A
FLAG (M2)-HRP conjugated	Sigma-Aldrich	A8592
gamma-H2AX	EMP Millipore	05-636-I
H2AX	Cell Signaling Technologies	2595S
BARD1 (E-11)	Santa Cruz Biotechnology	sc-74559
RBBP8	Santa Cruz Biotechnology	sc-271339
Spinophilin/Neurabin-II (D-7)	Santa Cruz Biotechnology	sc-373974
UIMC1	Abcam	ab-124763
BRIP1	Abcam	ab-180853
MLH1	Abcam	ab-92312
USP28	Abcam	ab126604
HA	Santa Cruz Biotechnology	sc-57592
BRCA2	EMP Millipore	OP95
RIF1	Cell Signaling Technologies	95558
I-SceI	Abcam	ab-216263
GAPDH	Abcam	ab-9485
Cell Culture Media		**Cat#**
High glucose Dulbecco's modified Eagle's medium (DMEM)	Corning	10-016-CV

DMEM and Ham's F-12 50/50	Corning	15-090-CV
RPMI1640	Corning	10-040-CV
Chemicals, Drugs, Peptides, and Enzymes		**Cat#**
Fetal Bovine Serum	Gibco	A3160502
Horse Serum	Thermo FIsher	16050-130
Penicillin/Streptomycin	Corning	MT30002CI
Gag-Pol-Tat-Rev		pJH045
VSV-G		pJH046
PolyJet DNA Transfection Reagent	SignaGen Laboratories	SL100688
8.5% PEG-6000	Sigma EMD Millipore	528877
Puromycin	Sigma	P8833
Blasticidin S HCl	Gibco	R21001
Doxycycline	Selleckchem	S4163
100X Halt™ Protease and Phosphatase Inhibitor Single-Use Cocktail, EDTA-Free	Thermo Scientific	78443
Benzonase	Sigma	E1014-25KU
LysC	Wako Chemicals	129-02543
Iodoacetamide (IAA)	BioUltra	I1149
Trypsin	Promega	V611X
6X SDS Sample Buffer	Alfa Aesar	J61337-AD
Hydrocortisone	Sigma-Aldrich	H0888-1G
Insulin Solution Human I9278	Sigma-Aldrich	501656853
Animal-Free Recombinant Human EGF	PeproTech	10781-696 (EA)
Cholera Toxin	Sigma-Aldrich	C-8052
Janus Green Stain	Abcam	ab111622
Invitrogen Nuclease-Free Water	Ambion	AM9938
16% Paraformaldehyde	Thermo Fisher	PI28908
Triton X-100	Sigma-Aldrich	9002-93-1
Lipofectamine 2000	Invitrogen	11668019
Lipofectamine RNAiMAX	Invitrogen	13778150
Opt-mem Reduced Serum	Gibco	31985070
Duolink In Situ Red Starter PLA Kit	Sigma-Aldrich	DUO92101
Cas9-NLS purified protein	MacroLab	
Laboratory equipment and other reagents		**Cat#**
0.45 µm PVDF filter	Millipore	MM_NF-SLHV033RS
Nest Tips C18	The Nest Group	SUM SS18V
Anti-FLAG M2 magnetic beads	Sigma-Aldrich	M8823
Anti-HA magnetic beads	Thermo Fisher	88836
Ubiquitin Remnant Motif (K-ε-GG) Antibody Bead Conjugate	Cell Signaling Technologies	5562
Ni-NTA Magnetic Agarose Beads	Qiagen	36111
Micro Bio-Spin chromatography Columns	Bio-Rad	7326204
7.5 % Mini-PROTEAN® TGX™ Precast Protein Gel	Bio-Rad	4561024
Trans-Blot Turbo Transfer System	Bio-Rad	
KwikQuant Ultra Digital ECL-solution	Kindle Biosciences, LLC	R1002
KwikQuant™ Imager	Kindle Biosciences, LLC	
KwikQuant Image Manager Software	Kindle Biosciences, LLC	
Echo Qualified Labcyte 384-well plates	Dharmacon	cat# PP-0200
Clear-bottom 96 Well Plates	Corning	CLS3904
Li-Cor Odyssey CLx	Li-Cor	9140

8-well Chamber Slide	ibidi	80826
SE Cell line 96-well nucleofector kit	Lonza	V4SC-1960
Nucleofector 4D system	Lonza	
Deposited Data		**Cat#**
Raw AP-MS and abundance MS files and their MaxQuant search files	Proteome Xchange Pride partner Repository	Identifier: PXD019639
Raw PTM (ub and ph) MS files and their MaxQuant search files	Proteome Xchange Pride partner Repository	Identifier: PXD025931
PPI network	NDEx	https://bit.ly/3y10JFY
Breast cancer protein-protein interaction network	doi:10.18119/N9BS4B	https://doi.org/10.18119/N9BS4B
Shared interactions between MCF7 and MDA-MB-231 cells	doi:10.18119/N9GG67	https://doi.org/10.18119/N9GG67
BRCA1 interactome (PPI>=0.65)	doi:10.18119/N9VP5B	https://doi.org/10.18119/N9VP5B
MCF10A_All (PPI>=0.9)	doi:10.18119/N9TS4P	https://doi.org/10.18119/N9TS4P
MCF7_All (PPI>=0.9)	doi:10.18119/N9Q01P	https://doi.org/10.18119/N9Q01P
MDA231_All (PPI>=0.9)	doi:10.18119/N9M89J	https://doi.org/10.18119/N9M89J
MCF10A_specific (PPI>=0.9)	doi:10.18119/N9701B	https://doi.org/10.18119/N9701B
MCF7_specific (PPI>=0.9)	doi:10.18119/N9389W	https://doi.org/10.18119/N9389W
MDA231_specific (PPI>=0.9)	doi:10.18119/N9ZG6K	https://doi.org/10.18119/N9ZG6K
Experimental Models: Cell Lines		**Cat#**
HEK293T	ATCC	CRL-3216
U2OS	Gunn and Stark, 2012	Jeremy Stark's laboratory
MDA-MB-231	ATCC	HTB-26
MCF7	ATCC	HTB-22
MCF10A	ATCC	CRL-10317
T47D	ATCC	HTB-133
SKBR3	ATCC	HTB-30
siRNAs and crRNAs		**Cat#**
STK11-siGENOME SMARTpool	Dharmacon	M-005035-02-0010
STK11 #1-siGENOME	Dharmacon	D-005035-01-0002
STK11 #3-siGENOME	Dharmacon	D-005035-05-0002
STRADA-siGENOME SMARTpool	Dharmacon	M-015407-00-0020
STRADA #2-siGENOME	Dharmacon	D-005343-03-0002
STRADA #3-siGENOME	Dharmacon	D-005343-05-0002
PIK3CA-siGENOME SMARTpool	Dharmacon	M-003018-03-0005
PTEN-siGENOME SMARTpool	Dharmacon	M-003023-02-0005
BPIFA1-siGENOME SMARTpool	Dharmacon	M-008613-00-0005
BPIFA1 #1-siGENOMEl	Dharmacon	D-008613-01-0002
BPIFA1 #2-siGENOMEl	Dharmacon	D-008613-02-0002
BPIFB1-siGENOME SMARTpool	Dharmacon	M-010095-00-0005
SCGB2A1-siGENOME SMARTpool	Dharmacon	M-019606-01-0005
SCGB2A1 #1-siGENOME	Dharmacon	D-019606-01-0002
SCGB2A1 #2-siGENOME	Dharmacon	D-019606-02-0002
PRR4-siGENOME SMARTpool	Dharmacon	M-012367-02-0005
MUC5B-siGENOME SMARTpool	Dharmacon	M-184282-00-0005
ZG16B-siGENOME SMARTpool	Dharmacon	M-015971-01-0005

ANXA1-siGENOME SMARTpool	Dharmacon	M-011161-01-0005
IRS1-siGENOME SMARTpool	Dharmacon	M-003015-01-0005
APOA1-siGENOME SMARTpool	Dharmacon	M-010994-00-0005
LTF-siGENOME SMARTpool	Dharmacon	M-019661-01-0005
PIK3R1-siGENOME SMARTpool	Dharmacon	M-003020-04-0005
PIGR-siGENOME SMARTpool	Dharmacon	M-017729-00-0005
PIP-siGENOME SMARTpool	Dharmacon	M-004904-00-0005
NTC siGENOME	Dharmacon	D-001210-02-50
USP28 #1-siGENOME	Dharmacon	D-006076-02-0010
USP28 #6-siGENOME	Dharmacon	CTM-661892 (UUGGUUUAGUGCUGUUAUUUU)
Spinophilin #4-siGENOME	Dharmacon	D-014932-02-0010
Spinophilin #5-siGENOME	Dharmacon	D-014932-03-0010
BRCA1-296-siGENOME	Dharmacon	CTM-554665 (GGAACCUGUCUCCACAAAGdTdT)
RIF1-siGENOME SMARTpool	Dharmacon	M-027983-01-0005
BRCA2-1949-siGENOME	Dharmacon	CTM-566149 (GAAGAAUGCAGGUUUAAUAdTdT)
USP28 crRNA #3	Dharmacon	CM-006076-03-0020 (CTGATGGAAGAGATCTTAAC
Spinophilin crRNA #3	Dharmacon	crRNA-556156 (TATCTTCGTCAAGACCGTGA)
NTC crRNA	Dharmacon	U-007501-01 (GATACGTCGGTACCGGACCG)
tracrRNA	Dharmacon	U-002005-50
Software and Algorithms		
FlowJo v106.1	FlowJo, LLC	https://www.flowjo.com/
Attune NxT Flow Cytometer	ThermoFisher	
Li-Cor Imaging Studio Software	Li-Cor	https://www.licor.com/bio/image-studio/
artMS	Bioconductor	https://www.bioconductor.org/packages/release/bioc/html/artMS.html
MSstats	Bioconductor	https://bioconductor.org/packages/release/bioc/html/MSstats.html
MaxQuant (version 1.6.2.10)	Jurgen Cox Lab	https://www.maxquant.org/
CompPASS (version 0.0.0.9000)	github	https://github.com/dnusinow/cRomppass/blob/master/R/comppass.R
SAINTexpress (version 3.6.1)	Sourceforge	https://sourceforge.net/projects/saint-apms/files/
InstantClue		http://www.instantclue.uni-koeln.de/